Journal of Thermal Analysis and Calorimetry, Vol. 75 (2004) 837–846

CADMIUM(II)BIS(OXALATO)COBALTATE(II)–PENTAHYDRATE
Thermal decomposition

N. Deb[*]

Department of Chemistry, North Eastern Regional Institute of Science and Technology, Nirjuli 791109, Itanagar, Arunachal Pradesh, India

(Received April 29, 2003; in revised form August 5, 2003)

Abstract

A mixed metal carboxylate, cadmium(II)bis(oxalato)cobaltate(II)pentahydrate, has been synthesized and characterized by elemental analysis, IR spectral, reflectance and X-ray powder diffraction studies. Thermal decomposition studies (TG, DTG and DTA) in air showed that the compound decomposed to $CdCoO_3$ at 370°C through the formation of an anhydrous compound at ~194°C. Finally, $CdCoO_2$ is generated at 1000°C. DSC study in nitrogen up to 550°C showed the formation of a mixture of CdO and Co_3O_4 as end products. The kinetic parameters have been evaluated for the dehydration and decomposition steps using four non-mechanistic equations, i.e., Freeman and Carroll, Coats and Redfern, Flynn and Wall, MacCallum and Tanner equations. Using seven mechanistic equations, the rate controlling processes of the dehydration and decomposition mechanism are also inferred. The kinetic parameters, ΔH and ΔS obtained from DSC are discussed. IR and X-ray powder diffraction studies identified some of the decomposition products. A tentative mechanism for the decomposition in air is proposed.

Keywords: kinetic parameters, mechanistic, oxalato, TG-DTA-DSC, thermal decomposition

Introduction

Attempts had been made [1] on the investigation of structure and magnetic properties of $Cu^{II}Ni^{II}$μ-oxalato mixed linear chain i.e., $NiCu(C_2O_4)_2\ 4H_2O$, which is the simplest one dimensional ordered bimetallic system with different electronic spins. Studies [2] on the thermal properties of co-precipitated zinc-copper oxalates in nitrogen indicated the formation of mixed oxide and copper metal as end product. The synthesis, structure and the magnetic properties of an ordered bimetallic $Cu^{II}Mn^{II}$ chain opened [3] a new perspective in the field of one-dimensional magnetic systems. The study on the dehydration/rehydration of ammonium tris oxalato aluminate [4] in the controlled atmosphere of flowing dinitrogen saturated with water vapour at room temperature using TG and XRD

* Author for correspondence: nidhubandeb@yahoo.com

1388–6150/2004/ $ 20.00

Akadémiai Kiadó, Budapest
Kluwer Academic Publishers, Dordrecht

techniques determined the stability domains of its trihydrate, dihydrate and anhydrous salt. Recently a report was made [5] on non-isothermal studies on mechanism and kinetics of thermal decomposition of cobalt(II)oxalate dihydrate, where the decomposition occurred in two steps; dehydration to anhydrous oxalate and next decomposition to Co and to CoO in two parallel reactions. The carboxylate coordination compounds with malate as ligand, $(NH_4)[Fe(C_4H_4O_5)(OH)_2]\cdot 0.5H_2O$, $[Ni(C_4H_4O_5)\cdot 3H_2O$ and $[Zn(C_4H_4O_5)]\cdot 5H_2O$ were found [6] to be decomposed to respective α-Fe_2O_3, NiO and ZnO through the intermediate formation of anhydrous malates, malonates and oxyacetates in iron and nickel compounds and hydroxocarbonate as intermediate in zinc compound. We have synthesized and investigated [7–9] the thermal decomposition of the compounds of the type $M[M(C_2O_4)_2]\cdot xH_2O$ (where *M*=same metal) with Co(II), Cd(II), Cr(III), Sb(III) and La(III), and found the different intermediates and end products in different atmosphere. Although there have been quite a few reports on the mixed two-metal carboxylate, so far oxalate of cadmium with cobalt had not been reported. As an extension of our work [10–13] on thermal properties of mixed metal carboxylate, where we used oxalate as ligand and keeping in view of the possibility of formation of metal oxide or mixed metal oxide and their possible catalytic applicability, we report here the characterization and thermal decomposition behaviour of $Cd[Co(C_2O_4)_2]\cdot 5H_2O$. A tentative scheme of the decomposition in air is also proposed.

Experimental

Preparation of the complex

The compound was prepared from cobalt(II) chloride by the similar method adopted earlier [12]. All the reagents used were AR grade. The chloride free cobalt hydroxide prepared from cobalt chloride was dissolved in glacial acetic acid and heated on a steam bath. Adding cadmium chloride followed by dropwise addition of saturated solution of oxalic acid separated a light pink precipitate. The precipitate was washed several times with distilled water and stored in a desiccator over calcium chloride. The water content was determined gravimetrically and metal contents were estimated using standard methods.

Elemental analysis was done with a Carlo Erba 1108 elemental analyzer. IR (200–4000 cm^{-1}) spectra of the compound and decomposition products were recorded on a Perkin Elmer IR 883 spectrophotometer. Diffuse reflectance spectrum was recorded with a Shimadzu UV-240 spectrophotometer. TG, DTG and separately DTA were carried out at 10°C min^{-1} in static air with a Shimadzu DT-30B thermal analyzer. The amount of sample taken was 6.67 mg in TG and 10.0 mg in DTA. DSC curves were recorded with a TA instrument DSC-2010 at a heating rate of 10°C min^{-1} up to 550°C in nitrogen. The sample mass was 7.28 mg. The ΔH (enthalpy change) of the processes was determined after integration of the peaks. The powder X-ray diffraction (XRD) pattern of the compound was taken using a Geigerflex microprocessor controlled automated Rigaku (Japan) X-ray diffractometer system D/Max IIIC. Model JDX-11P3A Jeol

diffractometer using Ni filter with CuK_α radiation at 35 kV and 10 mA in the wide angle $2°<2\theta<60°$ was used to take the powder-XRD pattern of the decomposition products.

The kinetics of decomposition

Kinetic parameters, such as activation energy (E^*), pre-exponential factor (A) and the order of reaction (n) of dehydration and decomposition steps were calculated from non-isothermal TG curves using different non-mechanistic equations, such as Freeman and Carroll [14], Coats and Redfern [15], Flynn and Wall [16], MacCallum and Tanner [17].

Several authors [18–21] have discussed evaluation of the mechanism of reaction using mechanistic equations. We have used the following kinetic expression [21].

$$\frac{\Delta \ln \alpha'}{\Delta \ln(1-\alpha)} = -\frac{E^*}{R}\frac{\Delta(1/T)}{\Delta \ln(1-\alpha)} + \frac{\Delta \ln f(\alpha)}{\Delta \ln(1-\alpha)} \quad (1)$$

where the terms have their usual meaning and $f(\alpha)$ is a function depending on the actual mechanism of the process.

A series of seven forms of $f(\alpha)$ are proposed [21] out of the possible mechanisms [19] of thermal decomposition. Thus a plot of $\Delta \ln \alpha' - \Delta \ln f(\alpha)/\Delta \ln(1-\alpha)$ *vs.* $\Delta(1/T)/\Delta \ln(1-\alpha)$ is a straight line whose slope is $-E^*/R$, irrespective of the form of $f(\alpha)$ employed. One can select the $f(\alpha)$ that best fits the actual mechanism of reaction corresponding to the intercept value close to zero. The actual mechanisms are as follows.

Mechanism	Rate-controlling process
D1	One-dimensional diffusion
D2	Two-dimensional diffusion
D3	Three-dimensional diffusion; Jander equation
D4	Three-dimensional diffusion; Ginstling–Brounshtein eq.
F1	Random nucleation
R2	Phase-boundary reaction (cylindrical symmetry)
R3	Phase-boundary reaction (spherical symmetry)

Further, to test the correctness and validity of the above conclusion regarding the identification of the actual mechanism of the process, the Arrhenius equation of the following type is used.

$$\ln \alpha' - \ln f(\alpha) = \ln(A/\beta) - E^*/RT \quad (2)$$

where the terms have their usual meaning. The slope, $-E^*/R$, and intercept, $\ln(A/\beta)$, can be obtained from the plot of $\ln \alpha' - \ln f(\alpha)$ *vs.* $1/T$ which is a straight line. It now follows that the mechanism proposed on the basis of the kinetic Eq. (1) is correct provided the E^* value obtained from the above plot of (2) turns out to be same.

Thus, we have evaluated the E^* from TG curves employing the kinetic Eqs (1) and (2) for seven forms of $f(\alpha)$ and thus inferred the rate controlling process for the dehydration and decomposition steps as described above. The details of the kinetic parameters calculated can be seen from Table 4.

Results and discussion

The light pink compound was insoluble in water or in common organic solvents. However, it decomposed in the presence of strong acid or alkali. The metal and elemental analysis conforms to a molecular formula, $Cd[Co(C_2O_4)_2]\cdot 5H_2O$. The IR peaks (Fig. 1 and Table 1) were assigned like earlier studies [9, 12, 13, 22] that show the presence of chelated $C_2O_4^{2-}$ groups as well as coordinated water molecules.

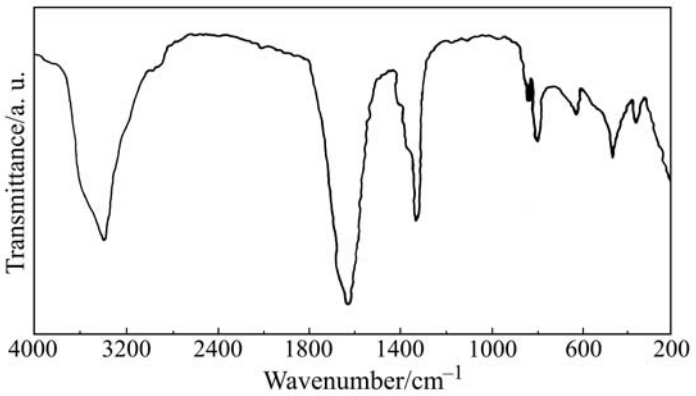

Fig. 1 IR spectrum of the complex, $Cd[Co(C_2O_4)_2]\cdot 5H_2O$

The electronic spectrum of solid sample displayed the bands around 20.000 and 22.200 cm^{-1} which are assigned to $^4T_{1g}(F)\rightarrow {}^4T_{1g}(P)$ and spin allowed transition, $^4T_{1g}(F)\rightarrow {}^4T_{2g}$, respectively, which indicates the octahedral cobalt environment [23]. The band at 45.450 cm^{-1} is due to intraligand $\pi\rightarrow\pi^*$ transition. The powder XRD pattern (Table 2) of the compound shows it crystalline in nature.

Table 1 Selected bands in the IR spectrum of the complex, $Cd[Co(C_2O_4)_2]\ 5H_2O$

IR band/cm^{-1}	Assignment
3000–3800 b	ν_{sy}(O–H)+ν_{asy}(O–H) or hydrogen bonding
1620 S	δ_{sy}(H–O–H)
1500–1800 b	ν_{asy}(C=O)
1330 S	ν_{sy}(C–O) and/or δ(O–C=O)
840 vvs, 800 m	ν(M–O) and/or δ(O–C=O) or coordinated water
630 m	Water of crystallization
460 m	ν(M–O) and/or ring deformation
360 m	δ(O–C=O) and/or ν(C–C)

b – broad; m – medium; S – strong; s – small; vs – very small

Table 2 Prominent lines in the X-ray powder diffraction pattern of $Cd[Co(C_2O_4)_2]\ 5H_2O$ and products from TG at 395 and 1000°C

$Cd[Co(C_2O_4)_2]\cdot 5H_2O$		Product at 395°C		Product at 1000°C	
d/Å	*I*(Rel)	*d*/Å	*I*(Rel)	*d*/Å	*I*(Rel)
9.849	61	4.260	91	8.762	57
4.881	100	4.222	68	7.472	65
2.835	77	4.024	70	6.736	56
2.317	67	3.795	95	6.490	59
2.137	65	3.468	70	4.398	51
1.902	67	3.371	80	3.885	51
1.634	55	2.946	100	3.091	42
1.517	51	2.792	59	3.030	33
1.252	46	2.601	49	2.961	47
1.140	43	2.479	68	2.864	45
1.087	43	2.065	45	2.771	37
1.028	44	1.890	56	2.700	97
0.913	39	1.832	62	2.460	78
0.874	38	1.682	77	2.437	49
0.849	41	1.598	48	2.412	34
0.835	41	1.560	41	2.339	100
0.818	43	1.500	37	2.280	61
0.809	40			2.129	96
0.798	38			1.830	34
0.786	41			1.655	69
				1.560	44
				1.510	70
				1.429	67
				1.315	52
				1.293	39

The thermal profiles (TG, DTG and DTA) of $Cd[Co(C_2O_4)_2]\cdot 5H_2O$ are shown in Fig. 2. In the TG curve the mass loss started from 65°C and an inclined slope up to 130°C indicates the removal of first three molecules of water. Another distinct TG slope between 160 and 194°C (mass loss, found 21%; calcd. 20.59%) indicates the complete elimination of the remaining two molecules of water. A change in DTG in the range 60–210°C with two responses corresponds to the whole dehydration process. A large endothermic peak in DTA between 80 and 160°C (ΔT_{min}=105°C) followed by another small endotherm in the range 160–220°C (ΔT_{min}=190°C) are accounted for the dehydration steps.

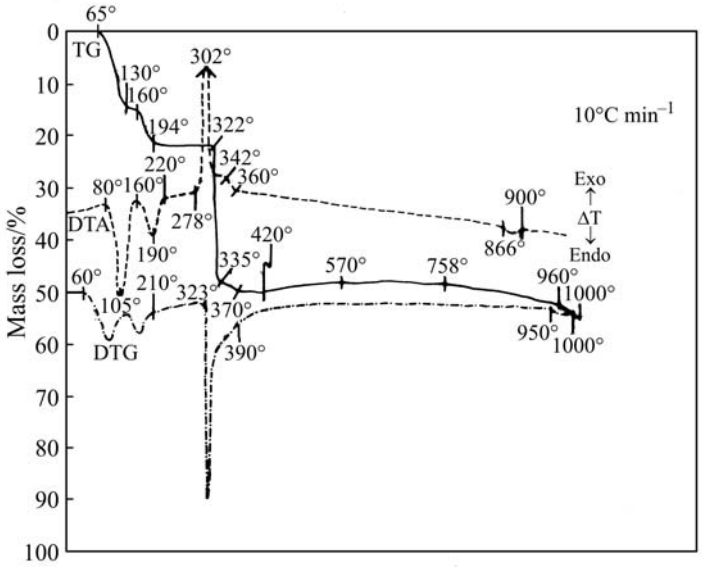

Fig. 2 TG, DTG and DTA curves of $Cd[Co(C_2O_4)_2]\cdot 5H_2O$ in air at 10°C min^{-1}

The kinetic parameters (activation energy (E^*), pre-exponential factor (A), and order of reaction (n)) calculated for both the dehydration steps from TG slope using four non-mechanistic equations [14–17] are included in Table 3. Differences in the values of E^* for the same step using different methods are observed like obtained by many workers [2, 9, 24, 25]. The variations may be due to the different methods based on different approaches and assumptions, and so those have different inherent limitations in the methods of calculation. The E^* of the step was calculated (Table 4) using seven mechanistic equations [18–21] and the rate controlling process of both the first and second dehydration steps is found to be random nucleation (F1). The mechanistic study suggested that the dehydration had taken place with higher E^* values in most of the mechanisms, whereas lower values are calculated adopting non-mechanistic equations. The anhydrous compound is stable up to 322°C in TG. The elemental, analytical and IR studies revealed that the pyrolysed species isolated in furnace up to 255°C was anhydrous and the coordinated oxalato group was retained. The most of the *d*-values in the XRD data of the species are similar to the precursor. The deaquated compound decomposes within a short temperature range as shown by a steep slope in TG in the range 322–335°C with a 48% mass loss. Further a small inclined slope from 335 to 370°C apparently suggests that the product formed at 335°C is slowly converted to $CdCoO_3$ (mass loss, found 50%; calcd. 49.86%). The XRD pattern of the black product obtained after independent pyrolysis up to 395°C (as the TG curve was stable up to 420°C) indicates [26] the contamination with traces of $CdCO_3$ and carbon along with the main product. Further, IR bands due to CO_3^{2-} group at 1360–1550, 1030 and 845 cm^{-1} gives credence to the presence of $CdCO_3$. The mass gain of 2% in the range 420–570°C may be due to the slow formation of carbide [9, 11] through the solid – gas reaction of evolved carbon monoxide in contact with the solid products which led disproportionation of CO(g) to C and CO_2(g). The free

unoxidised and unreacted carbon may also increase the mass of residue [13]. An exothermic peak between 278 and 360°C (ΔT_{max}=302°C) with a shoulder at the base of the peak at 342°C in DTA and a change in DTG (323–390°C) are accounted for the major decomposition. A part of CO(*g*) evolved during decomposition of anhydrous form is immediately oxidised to CO_2(*g*) by air accompanied by an exothermic peak in DTA around 302°C. The shoulder may be responsible for the change of product formed at 335°C in TG to $CdCoO_3$ at 370°C. The E^* value for the major decomposition step calculated using four non-mechanistic methods are found (Table 3) to be much higher than the dehydration step. The kinetic analysis of the TG data for E^* values (Table 4) using mechanistic equations showed dominance of kinetic control mechanism based on phase-boundary reaction having cylindrical symmetry (R2). Most of the E^* values (Table 4) calculated using mechanistic equations for the decomposition step are found to be much lower than the values calculated (Table 3) using non-mechanistic equations. The product is stable from 570 to 758°C in TG followed by a slight mass loss up to 1000°C through a break at 960°C. The 53% mass loss at 1000°C might be due to change to greenish coloured $CdCoO_2$ (mass loss, calcd. 53.52%) which is an intimate mixture of CdO and CoO (olive green). Corresponding to the break in TG at 960°C the DTG showed a change between 960 and 1000°C and DTA recorded a small endotherm in the range 866–900°C. The XRD data of the product isolated at 1000°C confirmed [26] the presence of CdO, CoO and carbide of cobalt. A trace of Co_3O_4 is also detected from the *d*-values. The other mismatched *d*-values may be correlated to $CdCoO_2$. The IR band at 654, 560 and 350 cm^{-1} of the residue further substantiate [27] the presence of Co_3O_4.

Table 3 Kinetic data evaluated by the methods (a) Freeman and Carroll, (b) Coats and Redfern, (c) Flynn and Wall, (d) MacCallum and Tanner equation

Step	Reaction	Method	E^*/kJ mol^{-1}	Order of reaction, *n*	A/s^{-1}
1	1st dehydration step	a	12.37	0.5	
		b	17.51		$8.3\ 10^4$
		c	7.32	0.5	
		d	16.09		$1.1\ 10^5$
2	2nd dehydration step	a	10.32	0.5	
		b	13.10		$6.2\ 10^3$
		c	6.94	0.5	
		d	12.02		$4.5\ 10^4$
3	Decomposition step	a	259.24	0.5	
		b	233.49		$8.2\ 10^{12}$
		c	247.21	0.5	
		d	248.17		$3.6\ 10^{29}$

The DSC profile (Fig. 3) in nitrogen shows three distinct endothermic peaks. The first endotherm (peak temperature, 87.35°C) which is for dehydration consisted

Table 4 Kinetic data evaluated by the seven mechanistic equations

Step	Mechanism	Form of $f(\alpha)$	(A)		(B)		Difference of E^* between (A) and (B)/ %
			Correlation coefficient/r	E^*/ kJ mol^{-1}	E^*/ kJ mol^{-1}	A/ s^{-1}	
1st dehydration step	D1	$1/2\alpha$	0.9876	830.57	652.58	$2.51\ 10^{56}$	21.43
	D2	$[-\ln(1-\alpha\ ]^{-1}$	0.9854	879.42	664.45	$1.69\cdot10^{57}$	24.44
	D3	$3/2(1-\alpha)^{2/3}[1-(1-\alpha\ \ ]$	0.9952	56.60	93.44	$3.80\cdot10^{8}$	39.43
	D4	$[3/2(1-\alpha^{-}\ \ ]^{-1}$	0.9924	461.43	391.54	$1.09\cdot10^{34}$	15.15
	F1	$(1-\alpha)$	0.9992	568.27	568.27	$6.03\cdot10^{49}$	00.00
	R2	$2(1-\alpha)^{1/2}$	0.9643	664.45	442.97	$1.48\cdot10^{38}$	33.33
	R3	$3(1-\alpha)^{2/3}$	0.9376	622.92	465.12	$8.51\cdot10^{39}$	25.33
2nd dehydration step	D1	$1/2\alpha$	0.9858	782.13	551.78	$7.12\cdot10^{47}$	29.45
	D2	$[-\ln(1-\alpha\ ]^{-1}$	0.9912	810.12	572.10	$3.40\cdot10^{51}$	29.38
	D3	$3/2(1-\alpha)^{2/3}[1-(1-\alpha\ \ ]$	0.9927	42.13	132.10	$2.30\cdot10^{6}$	68.11
	D4	$[3/2(1-\alpha^{-}\ \ ]^{-1}$	0.9837	358.40	290.00	$1.78\cdot10^{28}$	19.08
	F1	$(1-\alpha)$	0.9989	472.32	472.30	$4.20\cdot10^{34}$	00.00
	R2	$2(1-\alpha)^{1/2}$	0.9821	582.42	379.86	$7.12\cdot10^{31}$	34.78
	R3	$3(1-\alpha)^{2/3}$	0.9908	512.92	314.12	$6.10\cdot10^{28}$	38.76
Decomposition step	D1	$1/2\alpha$	0.9812	189.84	77.87	$1.21\ 10^{8}$	58.98
	D2	$[-\ln(1-\alpha\ ]^{-1}$	0.9235	315.62	75.50	$3.25\cdot10^{7}$	76.08
	D3	$3/2(1-\alpha)^{2/3}[1-(1-\alpha\ \ ]$	0.8998	192.69	64.37	$2.20\cdot10^{9}$	66.59
	D4	$[3/2(1-\alpha^{-}\ \ ]^{-1}$	0.9875	19.10	8.90	$5.37\cdot10^{2}$	5.34
	F1	$(1-\alpha)$	0.9821	15.50	8.74	$2.90\cdot10^{2}$	4.36
	R2	$2(1-\alpha)^{1/2}$	0.9990	9.13	9.13	$6.99\cdot10^{2}$	00.00
	R3	$3(1-\alpha)^{2/3}$	0.9213	9.23	34.36	$1.06\cdot10^{4}$	73.14

(A) Results obtained by using the seven mechanisms for the plot of $\Delta\ln\alpha'-\Delta\ln f(\alpha)/\Delta\ln(1-\alpha)$ *vs.* $\Delta(1/T)/\Delta\ln(1-\alpha)$, and (B) for the Arrhenius plot of $\ln\alpha'-\ln f(\alpha)$ *vs.* $1/T$. The underlined same values of E^* calculated by (A) and (B) indicates that the proposed mechanism (F1 and R2) are correct.

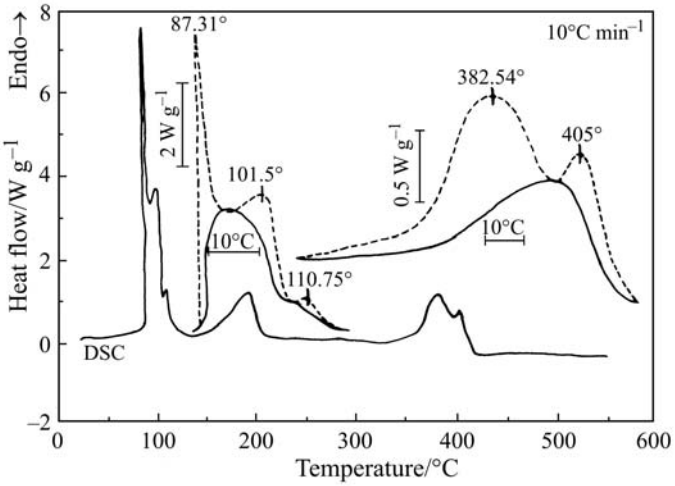

Fig. 3 DSC curves of $Cd[Co(C_2O_4)_2]\cdot 5H_2O$ in nitrogen at 10°C min^{-1}

of two shoulder peaks for the stepwise removal of water molecules. We enlarged the endotherm by enlarging the temperature axis, and the computed values of ΔH of the respective peaks (peak temperatures, 87.31, 101.50 and 110.75°C) for the stepwise release of water are found to be 36.17, 18.64 and 1.74 kJ mol^{-1}. The corresponding ΔS values of the steps are calculated to be 100.39, 49.77 and 4.55 kJ^{-1} mol^{-1}. Immediately after the dehydration step, another endothermic peak (peak temperature, 193.69°C) with large ΔH and ΔS values (85.74 and 183.72 Jk^{-1} mol^{-1}, respectively) suggests some rearrangement of anhydrous form which may take place very slowly and is quite stable. Finally, another endotherm (peak temperature, 382.94°C) recorded with a shoulder peak is for final decomposition in this study. The ΔH values of the enlarged main (peak temperature, 382.54°C) and shoulder peak (peak temperature, 405°C) are computed to be 51.23 and 12.01 Jk mol^{-1}, respectively. The corresponding ΔS values are calculated to be 78.14 and 17.71 Jk^{-1} mol^{-1}. The values of ΔH and ΔS are dependent on the area of the endotherm of the respective changes. The low value of enthalpy (ΔH) and entropy (ΔS) changes of the smaller peak suggest [18] the reduction and /or interaction phenomena rather than the decomposition. The product formed at 420°C is stable in nitrogen indicated by no further change of DSC profile. The mass loss of 44.64% of the annealed sample up to 550°C is attributed to the formation of a mixture of CdO and $0.5Co_3O_4$ as an end product (calcd. mass loss, 43.12%). The powder XRD confirmed [26] the presence of both the oxides.

The water vapour, carbon monoxide and carbon dioxide evolved during decomposition were identified by IR spectroscopy [22].

The above study suggests the following tentative mechanism for thermal decomposition in air.

$$Cd[Co(C_2O_4)_2]\cdot 5H_2O \xrightarrow{130^\circ C} Cd[Co(C_2O_4)_2]\cdot 2H_2O(s)+3H_2O(v) \xrightarrow{194^\circ C}$$

$$Cd[Co(C_2O_4)_2](s)+2H_2O(v) \xrightarrow{370^\circ C} CdCoO_3(s)+CdCO_3(s)+CoCO_3(s)(\text{trace})+$$

$$C(s)(\text{trace})+xCO(g)+yCO_2(g)\xrightarrow{420-570^\circ C}CdCoO_3(s)+CdCO_3(s)+CoCO_3(s)(\text{trace})+$$
$$Co_2C(s)(\text{trace})+C(s)(\text{trace})\xrightarrow{1000^\circ C}CdCoO_2(s)+CdO(s)+CoO(s)+Co_3O_4(s)+$$
$$Co_2C(s)(\text{trace})$$

* * *

The author thankful to Dr. S. D. Baruah, Regional Research Laboratory, Jorhat for the DSC profile.

References

1 M. Verdaguer, M. Julve, A. Michalowicz and O. Khan, Inorg. Chem., 22 (1983) 2624.
2 B. D. Dalvi and A. M. Chavan, J. Thermal Anal., 14 (1978) 331.
3 A. Gleizes and M. Verdaguer, J. Am. Chem. Soc., 103 (1981) 7373.
4 M. Ezahri, M. El Hadek, G. Coffy and B. F. Mentzen, J. Therm. Anal. Cal., 68 (2002) 207.
5 B. Małecka, E. Drozdz-Ciesla and A. Małecki, J. Therm. Anal. Cal., 68 (2002) 819.
6 L. Patron, O. Carp, I. Mindru, G. Marinescu and E. Segal, J. Therm. Anal. Cal., 72 (2003) 281.
7 N. Deb, P. K. Gogoi and N. N. Dass, J. Thermal Anal., 35 (1989) 27.
8 N. Deb, P. K. Gogoi and N. N. Dass, J. Instn. Chemists (India), 61 (1989) 185.
9 N. Deb, S. D. Baruah, N. Sen Sarma and N. N. Dass, Thermochim. Acta, 320 (1998) 53.
10 N. Deb, S. D. Baruah and N. N. Dass, Thermochim. Acta, 326 (1999) 43.
11 N. Deb, Thermochim. Acta, 338 (1999) 27.
12 N. Deb, S. D. Baruah and N. N. Dass, J. Therm. Anal. Cal., 59 (2000) 791.
13 N. Deb, J. Therm. Anal. Cal., 67 (2002) 699.
14 E. S. Freeman and B. Carroll, J. Phys. Chem., 62 (1958) 394.
15 A. W. Coats and J. P. Redfern, Nature, 201 (1964) 68.
16 J. H. Flynn and L. A. Wall, J. Res. Nat. Bur. Stand., A70 (1966) 6.
17 J. R. MacCallum and J. Tanner, Eur. Polym. J., 6 (1970) 1033.
18 N. Deb, S. D. Baruah, N. Sen Sarma and N. N. Dass, Thermochim. Acta, 329 (1999) 129.
19 W. W. Wendlandt, Thermal Methods of Analysis, Wiley, New York 1974, p. 45.
20 K. N. Ninan and C. G. R. Nair, Thermochim. Acta, 30 (1979) 25.
21 R. Lozano, J. Roman, J. C. Aviles, A. Moragues, A. Jerez and E. Ramos, Trans. Met. Chem., 12 (1987) 289.
22 K. Nakamoto, Infrared Spectra of Inorganic and Co-ordination Compounds 2nd Ed., Wiley, NewYork 1969, pp. 83, 89, 219, 245.
23 F. A. Cotton and G. Wilkinson, Advanced Inorganic Chemistry, Wiley, New York 1988, p. 730.
24 C. G. R. Nair and K. N. Ninan, Thermochim. Acta, 23 (1978) 161.
25 H. L. Saha and S. Mitra, Thermochim. Acta, 112 (1987) 275.
26 JCPDS, Inorganic Index to the Powder Diffraction File, 1971, 1601, Parklane, Pennsylvania.
27 F. F. Bentley, L. D. Smithson and A. L. Rozek, Infrared Spectra and Characteristic Frequencies, 300–700 cm^{-1}, Wiley, New York 1968.